RSC Advances

PAPER

View Article Online
View Journal | View Issue

Cite this: *RSC Adv.*, 2019, **9**, 34535

Synthesis of crosslinkable diblock terpolymers PDPA-*b*-P(NMS-*co*-OEG) and preparation of shell-crosslinked pH/redox-dual responsive micelles as smart nanomaterials†

Jingjing Sun,[ab] Zhao Wang,[bc] Amin Cao*[b] and Ruilong Sheng *[abd]

Received 4th July 2019
Accepted 25th September 2019

DOI: 10.1039/c9ra05082e

rsc.li/rsc-advances

Crosslinked polymer nanomaterials have attracted great attention due to their stability and highly controllable drug delivery; herein, a series of well-defined amphiphilic PDPA-*b*-P(NMS-*co*-OEG) diblock terpolymers (P1–P3) were designed and prepared *via* RAFT polymerization and were self-assembled into non-cross-linked (NCL) nanomicelles, which were further prepared into shell-cross-linked (SCL) micelles *via* cystamine-based *in situ* shell cross-linking. Using P3 as an optimized polymer, SCL-P3 micelles were prepared, which demonstrated remarkable pH/redox-dual responsive behaviour. For drug delivery, camptothecin (CPT)-loaded SCL-P3 micelles were prepared and showed much higher CPT-loading capability than their NCL-P3 counterparts. Notably, the SCL-P3 micelles showed good synergistic pH/redox-dual responsive CPT release properties, making them potential "smart" nanocarriers for drug delivery.

1. Introduction

Developing polymer-based drug delivery systems (DDSs) as biomaterials for anti-tumor drug delivery has attracted great attention in the past few decades. For achieving better controlled release properties, recently, many stimuli (pH,[1–3] bioreduction,[4,5] light,[6–8] enzyme[9,10]) responsive polymers have been developed as "smart" DDSs for drug delivery. It has been revealed that the micro-environment around tumor tissues has, in general, a pH value of 6.0–7.0,[11] lower than that of normal tissue (pH ~ 7.4). Inside tumor cells, endosomes/lysosomes also show much lower pH (4.5–6.0),[12] so the low pH value in tumor tissues/cells could be used as a target to design pH-responsive anti-tumor DDSs. For instance, Kataoka *et al.*[13] prepared some doxorubicin (DOX)-conjugated polymers with pH-responsive hydrazones, the hydrazone linkage was able to be cleaved inside lysosomes to release DOX under an acidic environment. Besides, some pH-responsive groups containing monomers including carboxylic acids (*e.g.* acrylic acid[14]) and tertiary amines bearing monomers (*e.g.* diethylaminoethyl methacrylate (DEAEMA)[15] and 2-(diisopropylamino)ethyl methacrylate (DPAEMA)[16–19]) were employed to prepare pH-responsive polymeric drug carriers. Licciardi *et al.*[20] prepared a series of PMPC-*b*-PDPA polymers containing hydrophilic 2-(methacryloyloxy) ethyl phosphorylcholine (MPC) residues and pH-sensitive hydrophobic 2-(diisopropyl amino)ethyl methacrylate (DPA) residues *via* ATRP polymerization, the loaded anti-tumor drugs tamoxifen and paclitaxel could be released under low pH of 5.0 *via* the protonation of PDPA block. Li *et al.*[21] prepared some worm-like pH-responsive PEG-*b*-PDPAEMA micelles to efficiently load photosensitizer chlorin E6, which could be employed as an efficient anti-cancer formulation in photodynamic therapy (PDT). Although a number of stimuli-responsive polymer micelles had been developed and applied in drug/gene delivery, nevertheless, the micelle architectures were connected by weak non-covalent interactions (hydrophobic, electrostatic, hydrogen bond, *etc.*), which made the micelles comparatively fragile to sustain against environmental changes (dilution, temperature, electrolytes, *etc.*), which could decrease the drug loading/releasing efficiency.[22]

Crosslinking has been regarded as an efficient method to increase the micelle stability by forming covalent bond-based condensed micelles. To date, shell-crosslinked,[23,24] core-crosslinked[25] and interface-crosslinked[26] micelles had been developed as stabilized nanocarriers for drug delivery. Among them, shell-crosslinked micelles take more advantages due to: (1) their relatively large and flexible hydrophobic core which enhanced drug loading efficiency;[27–29] (2) the crosslinked hydrophilic shell could be controlled by stimuli-responsive crosslinkers.[30,31] *e.g.* Jeong *et al.*[32] prepared some shell-crosslinked PEG-PAsp-PPhe

[a]*Department of Radiology, Shanghai Tenth People's Hospital, School of Medicine, Tongji University, Shanghai 200072, China*

[b]*Key Laboratory of Synthetic and Self-assembly Chemistry for Organic Functional Molecules, Shanghai Institute of Organic Chemistry, CAS, Lingling Road 345, Shanghai, 200032, China*

[c]*Department of Materials, Jinling Institute of Technology, Nanjing, 211169, China*

[d]*CQM – Centro de Química da Madeira, Universidade da Madeira, Campus da Penteada, 9000-390, Funchal, Portugal. E-mail: ruilong.sheng@staff.uma.pt*

† Electronic supplementary information (ESI) available. See DOI: 10.1039/c9ra05082e

micelles with acetal-containing crosslinker, the micelles showed high DOX loading capacity and stability even under the existence of sodium dodecyl sulfate (SDS), and pH-responsive DOX release. McCormick *et al.*[33] prepared PEO-*b*-P(DMA-*stat*-NAS)-*b*-PNIPAM micelles, which was then crosslinked with cystamine by reacting with the activated ester *N*-acryloxysuccinimide (NAS) group, the micelles were found stable in solution and dissociated under the existence of bioreductive agent DTT by break down of the disulfide linkages. Hu *et al.*[34,35] prepared redox/pH dual responsive PCL-*b*-P(OEGMA-*co*-MAEBA) and folic acid-modified micelles for camptothecin (CPT) delivery by using disulfide-bond and hydrazone linkage as the crosslinker, the loaded CPT micelles exhibited accelerated CPT release under acidic environment and/or the presence of bioreductive agent DTT. Zhai *et al.*[36] prepared CPT and DOX co-loaded crosslinked micelles *via* visible light-induced diselenide metathesis, which demonstrated controllable and combined CPT/DOX dual drug release manners in tumor-related redox microenvironments. Although these accomplishments had been made, rationally incorporate stimuli-responsive crosslinkers to achieve low cytotoxicity, high drug loading efficiency, especially multi (dual, triple or more)-stimuli responsive drug delivery manners, is still a challenge. Moreover, the structural-property relationships for the crosslinked multi-stimuli responsive micelles were need to be further investigated.

In this work, a series of PDPA-*b*-P(NMS-*co*-OEG) diblock terpolymers (P1–P3) were prepared *via* reversible addition–fragmentation chain transfer (RAFT) polymerization and were characterized, which self-assembled in solution to form non-cross-linked (NCL) nanomicelle (sizes: 30–90 nm), then the NCL micelles were *in situ* crosslinked with cystamine to prepare shell-cross-linked (SCL) micelles with pH-responsive PDPA core and redox-responsive disulfide-containing shell. Using the optimized $PDPA_{33}$-*b*-P(NMS_{22}-*co*-OEG_{25}) P3-micelles as the model, the pH/redox-dual responsive properties were studied by DLS and NMR. For drug delivery application, the antitumor drug camptothecin (CPT)-loaded P3-NCL and P3-SCL micelles were prepared (Scheme 1) and the related drug loading efficiency, pH/redox-dual responsive behaviors were studied by fluorescence spectrometer.

2. Experimental

2.1. Materials

Methacryloyl chloride (95%) was purchased from Shanghai Darui Finechem Reagent Co., Ltd. (China). *N*-Hydroxysuccinimide (NHS, 98%), 2-(diisopropyl-amino)ethyl methylacrylate (DPA, 99%), oligoethylene glycol methacrylate (OEG, 98%), cystamine dihydrochloride (98%) and camptothecin (98%) were obtained from Shanghai Energy Chemical Reagent Co., Ltd. (China). 1,4-Dioxane was dehydrated by refluxing with sodium and purified by distillation before use. 2, 2-Azobis(isobutyronitrile) (AIBN) was purchased from Shanghai Sinopharm Chemical Reagent Co., Ltd. (China) and was purified by re-crystallization in anhydrous ethanol. 4,4′-Azobis(4-cyanovaleric acid) (98%) was purchased from by Sigma & Aldrich. 0.1 M phosphate buffer solution (PBS 1×) was purchased

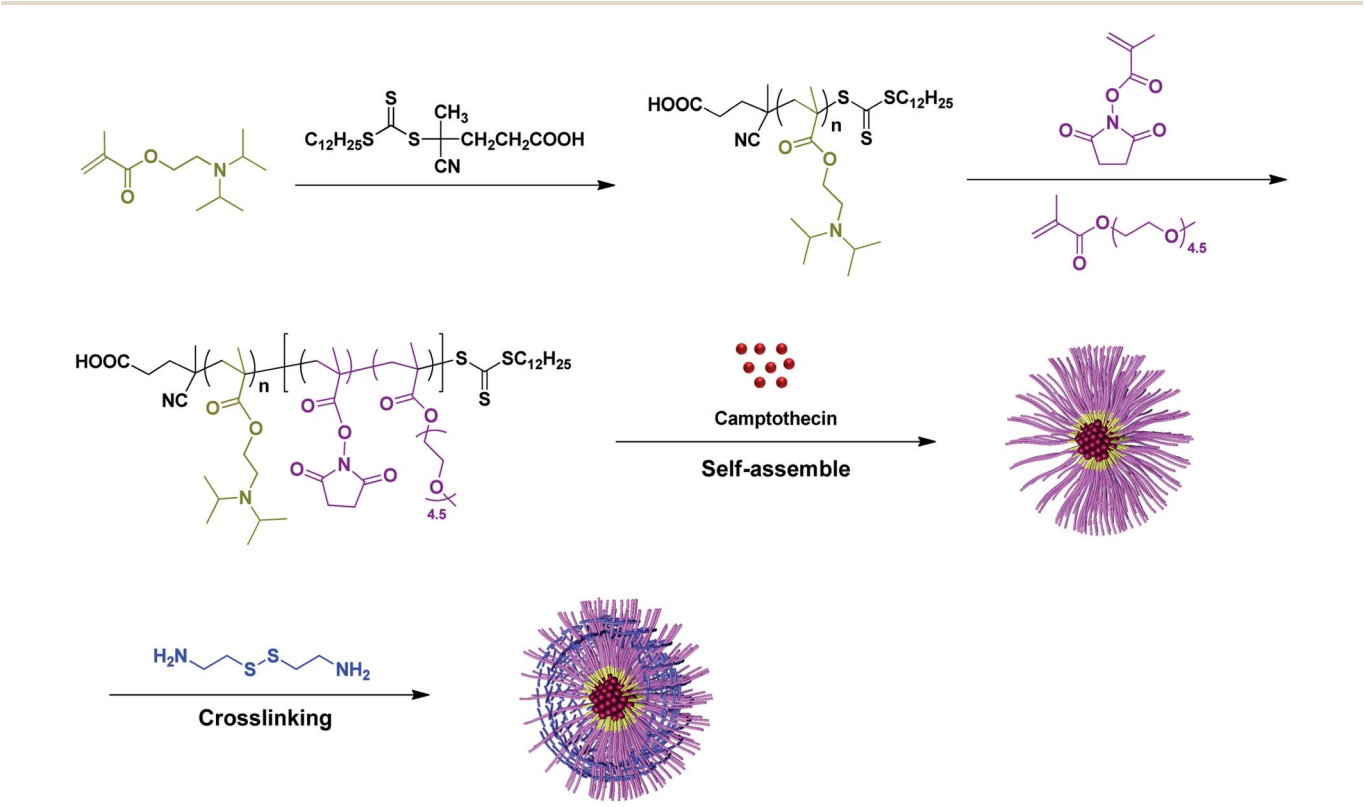

Scheme 1 Preparation of shell crosslinked micelles with pH-responsive core and redox-responsive shell *via* assembly of amphiphilic diblock terpolymer PDPA-*b*-P(NMS-*co*-OEG) and subsequent shell-cross linking with cystamine.

from Hangzhou Genom Co. Ltd. (China). All other chemicals and solvents were of analytical grade and were used as received.

2.2. Synthesis of PDPA-*b*-P(NMS-*co*-OEG) copolymers

2.2.1. Synthesis of macromolecular chain transfer agent PDPA. 2-(Diisopropylamino)ethyl methylacrylate monomer (3.2 g, 14.96 mmol), 2-(dodecylsulfanyl thiocarbonyl)-4-cyanovaleric acid (98 mg, 0.244 mmol), AIBN (8 mg, 0.0496 mmol) dissolved in 5 mL anhydrous dioxane was added into a dried Schlenk tube equipped with a magnetic stirrer bar. The mixture was deoxygenated by freeze–pump–thawing for three times and then immersed into an oil bath thermostated at 70 °C for 3 h. The reaction was quenched by cooling in liquid nitrogen and exposed to the air. The reaction solution was added dropwise into cooled diethyl ether, washed with 150 mL cooled methanol for three times, and dried under vacuum at 30 °C for 24 h to get the macromolecular chain transfer agent $PDPA_{33}$ as a yellow solid with a medium monomer conversion rate (75%).

^{1}H NMR (300 MHz, $CDCl_3$, δ in ppm): 3.84 (OCH_2CH_2N, 2*n*H, s), 2.99 ($-NCH(CH_3)_2$, 2*n*H, s), 2.62 (OCH_2CH_2N, 2*n*H, s), 2.25–1.60 (CH_2–CCH_3, 2*n*H, brm), 1.00 ($-CH(CH_3)_2$, 12*n*H, s), 0.89 ($-CH_2CH_3$, 3H, s).

FT-IR (in cm^{-1}): 2963, 1728, 1472, 1392, 1361, 1265, 1146, 1063, 1029, 983, 751.

2.2.2. Synthesis of PDPA-*b*-P(NMS-*co*-OEG) copolymers. Macromolecular reversible addition–fragmentation chain transfer (Macro-RAFT) agent PDPA (79 mg, 0.011 mmol), NMS monomer (35 mg, 0.191 mmol), OEG monomer (49 mg, 0.163 mmol), AIBN (0.6 mg, 0.0037 mmol) dissolved in 1.5 mL anhydrous dioxane was added into a dried Schlenk tube equipped with a magnetic stirrer bar. The mixture was deoxygenated by freeze–pump–thawing for three times and then immersed into an oil bath thermostated at 80 °C for 24 h. The reaction was quenched by cooling in liquid nitrogen and exposed to the air. The reaction solution was added dropwise into cooled hexane, washed with 150 mL cooled hexane for three times, and dried under vacuum at 30 °C for 24 h to obtain the PDPA-*b*-P(NMS-*co*-OEG) (P1) copolymers as yellow solid (95 mg). P2 and P3 copolymers were obtained by using the same protocol except changing the NMS (60 mg, 0.327 mmol for P2) and OEG feeding amount (70 mg, 0.232 mmol for P3), respectively.

^{1}H NMR (300 MHz, $CDCl_3$, δ in ppm): 4.32–3.80 (m, $-COOCH_2CH_2O$), 3.60 (d, $-COOCH_2CH_2O$), 3.38 (s, $-OCH_3$), 2.99 (s, $-NCH(CH_3)_2$), 2.82 (s, $-COCH_2CH_2CO-$), 2.63 (s, $-NCH_2CH_2-$), 2.36–1.69 (brm, $-CH_2-CCH_3$), 1.42–1.20 (brm, $-CH_2-$, $-CH_2CCH_3$), 1.01 (s, $-CH(CH_3)_2$), 0.85 (d, $-CH_2CH_3$).

FT-IR (in cm^{-1}): 2970, 2943, 2875, 1807, 1780, 1738, 1454, 1360, 1248, 1199, 1110, 1029, 953, 854.

2.3. Instrumental characterization of the synthesized monomers and polymers

2.3.1. NMR spectrum. ^{1}H NMR spectrum were conducted on a Varian-300 FT-NMR spectrometer at 300.0 MHz for proton nuclei, and ^{13}C NMR was implemented on a Bruker Avance-400 NMR spectrometer, operating at 100.0 MHz for ^{13}C nuclei, tetramethylsilane (TMS) was used as internal chemical shift reference in all NMR measurement.

2.3.2. FT-IR spectra. FT-IR spectra were recorded on a Bio-Rad FTS-185 spectrometer at room temperature in the wavenumbers ranging from 4000 to 500 cm^{-1} with 4 cm^{-1} spectral resolution (64 times scanning). Samples were dissolved in organic solvent (chloroform or pyridine) and casted on potassium bromide (KBr) pellets by evaporation of the solvent.

2.3.3. Gel permeation chromatography (GPC). Average molecular weights (M_n, M_w) and polydispersity index (M_w/M_n) of the synthesized protected glycopolymer precursors were measured at 35 °C on a PerkinElmer 200 GPC equipped with a refractive index detector (RI). THF was utilized as the eluent at a flowing rate of 1.0 mL min^{-1}, and a series of commercial polystyrene standards (Polymer laboratories, UK) with narrow molecular weight distribution were applied to calibrate the GPC elution traces.

2.4. Measurement of critical micelle concentration (CMC)

Pyrene was utilized as a fluorescence probe to determine the CMC of PDPA-*b*-P(NMS-*co*-OEG) copolymers. Pyrene/dichloromethane solution (0.02 mg mL^{-1}, 10 μL) was added into a 10 mL bottle and stay overnight to evaporate the dichloromethane, and the PDPA-*b*-P(NMS-*co*-OEG) polymer solution (2 mL, 1×10^{-4} to 5×10^{-1} mg mL^{-1}) with ultrasonic treatment for 10 min to give a pyrene/polymer solution, then equilibrated at room temperature in dark for 24 h before measurement. Then the fluorescence spectrum were recorded using a fluorescence spectrophotometer (F-7000, Hitachi, Japan) with the excitation wavelength of $\lambda_{ex} = 395$ nm and scan wavelength ranging from 300 to 360 nm. Fluorescence intensity ratio (I_{394}/I_{374}) was calculated and plotted as a function of copolymer concentration. CMC for each copolymer was determined at an inflection point of the plot.

2.5. Preparation of the non-cross-linked (NCL) micelles

First, each synthesized PDPA-*b*-P(NMS-*co*-OEG) polymer (10.0 mg) was dissolved in 2 mL tetrahydrofuran, 16 mL phosphate buffer solution (PBS, pH 7.4, 10 mM) was added dropwise into the mixture under vigorous stirring for 12 h. The NCL micelles was dialyzed against PBS using a pre-swollen cellulose dialysis membrane (MWCO 3500) for 48 h (the PBS was replaced in every 8 h) to remove the residual organic solvent.

2.6. Preparation of the shell-cross-linked (SCL) micelles

0.01 mM cystamine dihydrochloride aqueous solution was added into as-prepared NCL polymer micelles (the molar ratio of cystamine and NMS activated ester group was set as 1 : 2, pH 7.5–8) and stirred at room temperature for 24 h, then the SCL micelles was dialyzed against 0.01 M PBS using a pre-swollen cellulose dialysis membrane (MWCO 3500) for 24 h (the PBS was replaced in every 4 h).

2.7. Preparation of camptothecin (CPT)-loaded NCL and SCL micelles

First, $PDPA_{33}$-*b*-P(NMS_{22}-*co*-OEG_{25}) polymer (P3, 10.0 mg) was dissolved in 1 mL THF, camptothecin (1.0 mg, 10% w/w) dissolved in 1 mL DMSO and was then mixed with the THF solution polymer, 18 mL phosphate buffer solution (PBS, pH = 7.4, 10 mM) was added dropwise into the mixtures. Half amount (10 mL) of CPT/PDPA-*b*-P(NMS-*co*-OEG) copolymer solution was then dialyzed in deionized water by using a pre-swollen cellulose dialysis membrane (MWCO 3500) for 24 h to obtain the CPT-loaded NCL-P3 micelles. At the same time, another half (10 mL) of CPT/PDPA-*b*-P(NMS-*co*-OEG) copolymer solution was added with 0.01 mM cystamine hydrochloride aqueous solution (the molar ratio of cystamine and NMS activated ester group was preset as 1 : 2) and stirred at room temperature for 24 h, then the mixture was dialyzed against 0.01 M PBS using a pre-swollen cellulose dialysis membrane (MWCO 3500) for 24 h (the PBS was replaced in every 4 h) to get the CPT-loaded SCL-P3

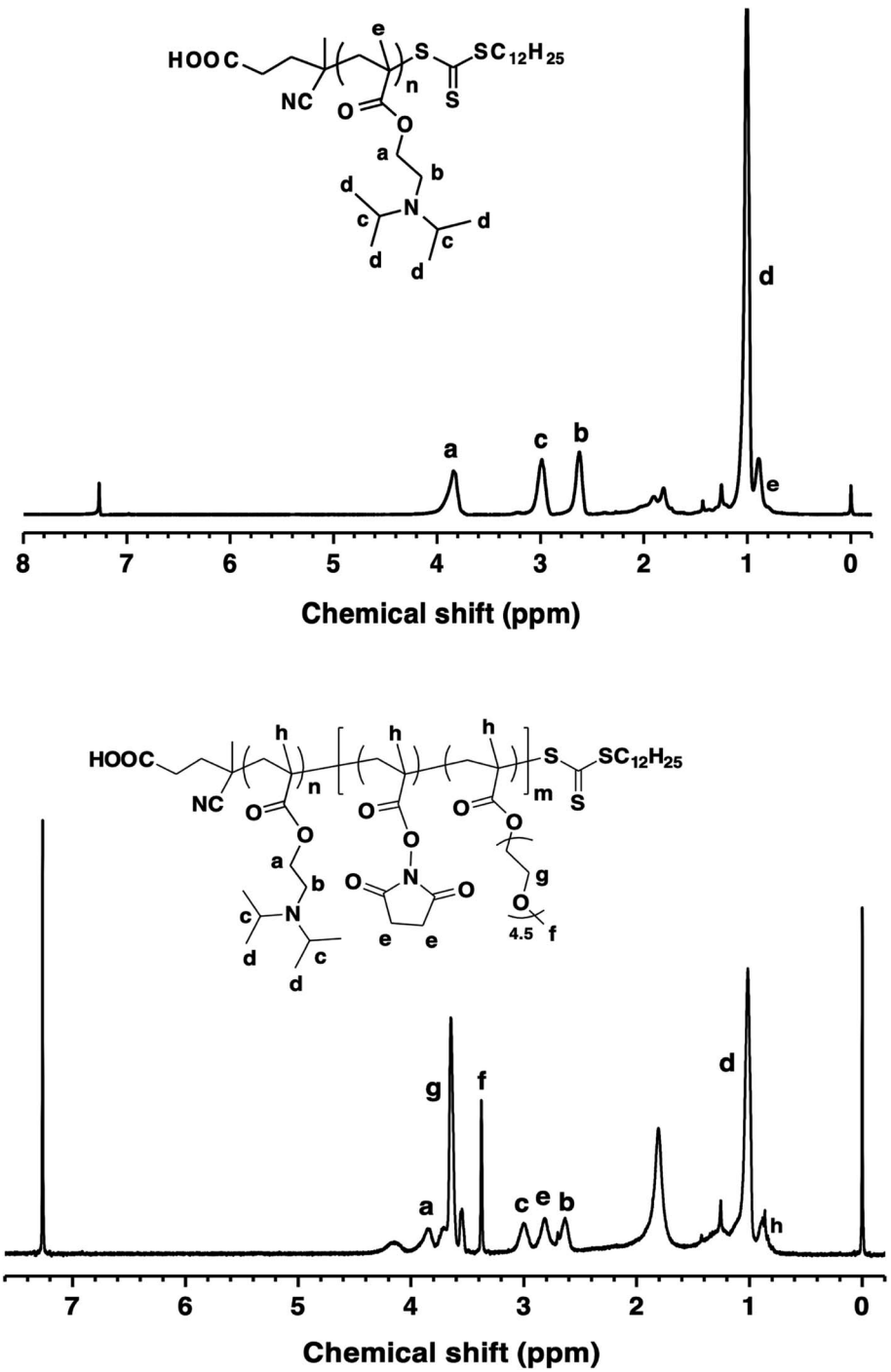

Fig. 1 ^{1}H NMR spectrum of the (top) $PDPA_{33}$ Macro-RAFT agent and (bottom) diblock terpolymer $PDPA_{33}$-*b*-P(NMS_{22}-*co*-OEG_{25}) (P3).

micelles. Finally, the free CPT was removed through 0.45 μm filter membrane.

2.8. Measurement of drug loading content and drug loading efficiency

CPT loading level was measured by UV-vis spectrophotometer (UV-2800, Hitachi, Japan).[37] Lyophilized CPT-loaded micelles were re-dissolved in DMF and the concentration was calculated according to a standard curve of pure CPT/DMSO solution. Drug loading content (DLC) and drug loading efficiency (DLE) were determined according to the following formulas:

$$\text{DLC (wt\%)} = \frac{\text{Weight of loaded drug}}{\text{Weight of loaded drug and polymers}} \times 100\%$$

$$\text{DLE (\%)} = \frac{\text{Weight of loaded drug}}{\text{Weight of drug in feed}} \times 100\%$$

where the weight of drug in feed represents the total amount of CPT added into the system.

The standard curve of CPT concentration-UV absorption: CPT dissolved into DMF to prepare the solution with various predetermined concentrations, the standard curve was obtained by plotted the absorbance of CPT at $\lambda = 365$ nm against various predetermined concentrations ($R = 0.99982$).

2.9. Release of CPT from the CPT-loaded NCL and SCL micelles

In brief, each CPT-loaded NCL-P3 and SCL-P3 micelles solution (2.5 mL) was transferred into a cellulose dialysis membrane (MWCO 3500), which was individually immersed into 40 mL of various buffer solution (10 mM PBS, pH 7.4; 10 mM PBS, 10 mM GSH, pH = 7.4; 10 mM acetic acid-sodium acetate (ABS), pH 5.0; 10 mM acetic acid-sodium acetate (ABS), 10 mM GSH, pH 5.0) and following gentle shaking of 150 rpm at 37 °C. The uncross-linked micelle solution (2.5 mL) under 40 mL of 10 mM PBS (pH = 7.4) was used as the control. At predetermined time intervals, 2 mL release media was taken out for UV-vis analysis and an equal volume of fresh media was added to maintain the dialysis conditions. The *in vitro* release of CPT was analyzed using a UV-vis spectrophotometer and calculated according to the calibration curve. The release experiments were conducted in triplicate at each pH values.

2.10. MTT assay

The cytotoxicity of NCL-P3 and SCL-P3 micelles were evaluated by MTT assay. H1299 cells were seeded in 96-well cell culture plates at the density of 8×10^3 cells per well, and 100 μL RPMI 1640 medium containing 10% FBS was added into each well and cultured for 24 h at 37 °C and 5% CO_2. After removing the original medium, 100 μL of micelles solution with different concentration was added and cultured for another 24 h. Then, 20.0 μL of 5.0 mg mL^{-1} MTT working solution was added to each well, and incubated for 2 h. After removing the medium, 100 μL of DMSO was added to each well to dissolve the formazan crystals. The cell viability was tested through the Biotek ELX 800 microplate reader.

3. Results and discussion

3.1. Synthesis and characterization of the diblock terpolymers PDPA-*b*-P(NMS-*co*-OEG)

The synthesis routes of the diblock terpolymers PDPA-*b*-P(NMS-*co*-OEG) were shown in Scheme 1. First, monomer 2-(diisopropylamino)ethylmethyl-acrylate (DPA) was polymerized (70 °C, in 1,4-dioxane) by using chain transfer agent 2-(dodecylsulfanylthiocarbonyl)-4-cyanovaleric acid with AIBN as the initiator, to prepare the Macro-RAFT agent PDPA. As shown in Fig. 1 and Table 1, the ^{1}H NMR peaks at 3.92, 2.98, 2.65 and 1.08 ppm were identified as the proton signals of DPA in the side chain of Macro-RAFT agent PDPA. Before purification, the polymerization mixture was tested by NMR for calculation of monomer conversion. The double bond signal ($\delta = 5.60$ ppm and 6.20 ppm) of DPA monomer (Fig. S1†) disappeared, which was converted to the Macro-RAFT agent $PDPA_{33}$ with a medium monomer conversion ratio (~75%). The degree of polymerization (DP) was calculated to be 33 according to the monomer feeding ratio and monomer conversion. GPC shows the purified $PDPA_{33}$ polymer has low molecular weight distribution (M_w/M_n, PDI = 1.16). The low PDI value of the Macro-RAFT agent $PDPA_{33}$ could benefit the preparation of structural-defined diblock terpolymers by subsequently integrating second block chain onto *via* RAFT polymerization.

Then the reactive monomer *N*-hydroxysuccinimide methacrylate (NMS) was synthesized (S1†) and characterized (Fig. S1†), which was then RAFT polymerized with a hydrophilic oligoethylene glycol methacrylate (OEG) monomer at 80 °C by using the as-synthesized Macro-RAFT agent $PDPA_{33}$ with AIBN as the

Table 1 Molecular characteristics of the synthesized PDPA and PDPA-*b*-P(NMS-*co*-OEG) copolymers

Sample	Composition	DPA cont[a]	NMS cont[b]	$M_{n,NMR}$[c]	$M_{n,GPC}$[d]	$M_{w,GPC}$[d]	M_w/M_n[d]
P0	$PDPA_{33}$	—	—	7400	7000	8100	1.16
P1	$PDPA_{33}$-*b*-P(NMS_{22}-*co*-OEG_{19})	40.4%	41.4%	16 300	11 700	17 200	1.47
P2	$PDPA_{33}$-*b*-P(NMS_{30}-*co*-OEG_{19})	37.1%	49.1%	17 800	13 200	18 300	1.39
P3	$PDPA_{33}$-*b*-P(NMS_{22}-*co*-OEG_{25})	36.4%	34.9%	18 100	14 600	20 400	1.40

[a] Weight percentage of DPA moieties in the PDPA-*b*-P(NMS-*co*-OEG) copolymers are determined by the formula: $DP_{(DPA)} \times M_{w(DPA)}/M_{w(polymer)}$. [b] Data mean weight percentage of NMS moieties in the hydrophilic block are determined by the formula: $DP_{(NMS)} \times M_{w(NMS)}/M_{w(hydrophilic\ part)}$. [c] Data were calculated from ^{1}H NMR spectra. [d] Molecular weights and their distribution were measured at 35 °C by GPC with THF as the eluent and calculated with polystyrene standard.

initiator, to prepare diblock terpolymers PDPA-*b*-P(NMS-*co*-OEG)s (P1–P3), in which the hydrophobic/hydrophilic ratio and reactive NMS ester groups could be controlled by changing the feeding ratio of NMS and OEGMA monomers. The P1–P3 polymer structures were further characterized by ^{1}H NMR and FT-IR spectra, the ^{1}H NMR spectra (P3) was shown in Fig. 1, it could be clearly seen that the proton signals (δ = 2.82 ppm (H_e, –CH_2 of NMS); δ = 2.63 ppm (H_c, –CH_2 of DPA) and δ = 3.38 ppm (H_f, –CH_3 of OEG)) on the diblock ternary polymer PDPA-*b*-P(NMS-*co*-OEG). The ^{1}H NMR and GPC characterization results of the Macro-RAFT agent $PDPA_{33}$ (P0) and the synthesized diblock terpolymer PDPA-*b*-P(NMS-*co*-OEG) were shown in Table 1, the medium molecular weight distribution (PDI 1.39–1.54) indicated that the PDPA-*b*-P(NMS-*co*-OEG) polymers with comparatively defined structures. The results demonstrated that the diblock terpolymer PDPA-*b*-P(NMS-*co*-OEG) with the reactive NMS ester could be synthesized and stably obtained through two-steps RAFT polymerization.

3.2. Preparation and characterization of the NCL and SCL micelles

In order to study the solution self-assembly behaviors of the as-prepared PDPA-*b*-P(NMS-*co*-OEG) polymers, the critical micelle concentration (CMC) of P1–P3 was measured by fluorescence spectra using pyrene as the fluorescence probe, the CMC values were obtained by plotting of the fluorescence intensity ratio (I_{337}/I_{333}) *versus* mass concentration of the PDPA-*b*-P(NMS-*co*-OEG) polymers (Fig. S2,† P3 as the example), the CMC results were shown in Table 2, it could be seen that the CMC value increased (5.2–8.8 mg L^{-1}, P1 < P3 < P2) with the increasing of the hydrophilic NMS and OEG ratios. The CMC results indicated that the PDPA-*b*-P(NMS-*co*-OEG) polymers maybe assemble into micelles with the hydrophobic PDPA "core" and hydrophilic P(NMS-*co*-OEG) "shell" structure in aqueous solution. Then the non-crosslinked (NCL) micelles were prepared and characterized by DLS, with the increasing of OEG ratio, the particle size dropped from 87.1 to 45.3 nm, due to the "shielding effect" of the hydrophilic OEG block. The above-prepared NCL micelles were further crosslinked with cystamine, a redox-responsive linker, to prepare the shell-crosslinked (SCL) micelles through the coupling reaction between amino groups in cystamine linker and reactive NMS ester groups (cystamine : NMS moiety, 1 : 2 molar ratio) in NCL micelles. After crosslinking with cystamine, it could be seen that the average particles size of the SCL (P1, P2 and P3) micelles maintained (SCL-P1, 85.1 nm) or slightly increased (SCL-P2, 89.9 nm; SCL-P3, 54.9 nm) than their NCL counterparts, which might due to the stabilization effect of hydrophobic PDPA "core" (Table 2).

It is known that smaller nanoparticles have relatively larger surface area, high drug loading efficiency, longer circulation half-life, as well as efficient cellular uptake. Herein, we chose P3, the small size micelle-forming polymer, as an example, for further study the related physico-chemical (aggregation, pH/redox-responsive and camptothecin loading/releasing) properties.

3.3. Study of the physico-chemical properties of the NCL-P3 and SCL-P3 micelles

The NCL-P3 and SCL-P3 micelles (freeze-dried micelle samples) were characterized with Fourier transform infrared spectroscopy (FT-IR), as shown in Fig. 2, compare to the NCL-P3 (a), the SCL-P3 micelles (b) showed obvious absorption peaks of amide (–CONH–) bonds at 3289 (ν_{-OH}), 1651 (ν_{C-O}) and 1546 cm^{-1} (ν_{C-O}), indicating that the SCL-P3 micelles were successfully prepared by using cystamine as the crosslinker. Moreover, the DLS curves of NCL-P3 and SCL-P3 (Fig. 3) showed slight particle size increasing of NCL-

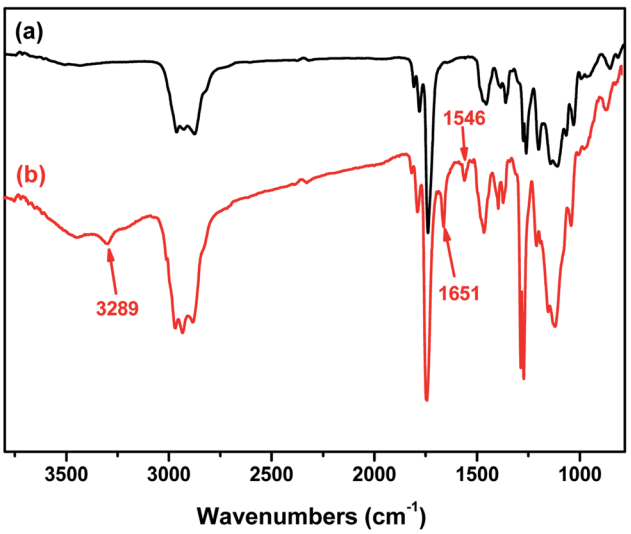

Fig. 2 Comparison of the FTIR spectra of the $PDPA_{33}$-*b*-P(NMS_{22}-*co*-OEG_{25}) (P3) micelles before (a) and after (b) shell cross-linking.

Table 2 Characteristics of non-crosslinked (NCL) and shell-crosslinked (SCL) PDPA-*b*-P(NMS-*co*-OEG) micelles

	NCL micelles			SCL micelles	
Sample	CMC[a] (mg L^{-1})	Size[b] (nm)	PDI[b]	Size[b] (nm)	PDI[b]
P1	5.2	87.1 ± 2.3	0.07 ± 0.07	85.1 ± 11.9	0.26 ± 0.11
P2	8.8	68.2 ± 0.8	0.10 ± 0.01	89.9 ± 8.9	0.24 ± 0.04
P3	7.3	45.2 ± 0.9	0.21 ± 0.02	54.9 ± 2.5	0.26 ± 0.04

[a] Determined with pyrene as a fluorescence probe. [b] Data were measured with Zetasizer Nano-ZS DLS (Malvern Instruments) at 25 °C in PBS solution.

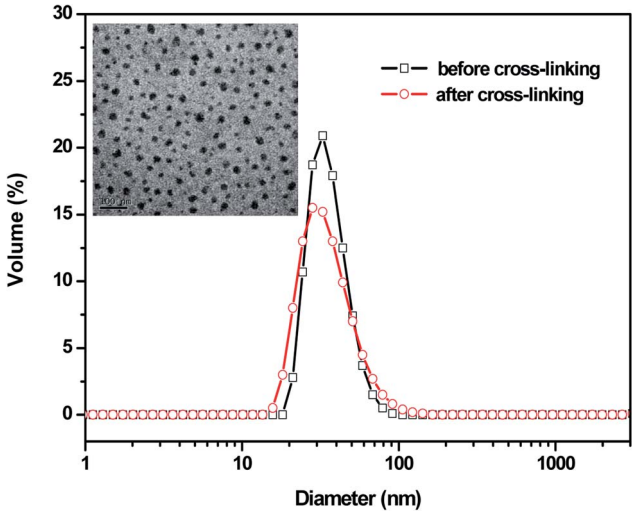

Fig. 3 Particle sizes and their distribution of the $PDPA_{33}$-*b*-P(NMS_{22}-*co*-OEG_{25}) (P3) micelles before and after shell cross-linking reaction. Inset: TEM images of the SCL-P3 micelles.

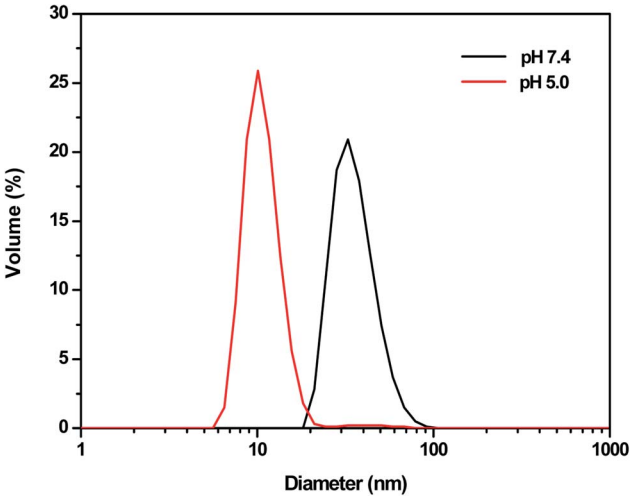

Fig. 4 Particle size and distribution of the NCL-P3 micelles under pH 7.4 and 5.0 by DLS.

P3 micelles after cystamine crosslinking, the comparatively low PDI (0.26) of the as-prepared SCL-P3 micelles implied that intra-micellar crosslinking occurred in NCL-P3 micelles instead of inter-micellar crosslinking, which made them good candidates for practical application. The morphology of SCL-P3 were observed by TEM imaging (Fig. 3, inset), it could be seen that the SCL-P3 micelles were homogenous spherical nanoparticles with average diameter of 30–70 nm, which is in accordance with the DLS results.

3.4. The stimuli-responsive properties of NCL-P3 and SCL-P3 blank micelles

Based on the above result, we further studied the stimuli-responsive property of NCL-P3 and SCL-P3 micelles. It has been reported that the hydrophobic PDPA have poor water solubility under neutral and basic conditions, while its water solubility would be greatly improved under acidic conditions due to the protonation of tertiary amino groups (iPr_2N) on PDPA,[17] which may bring pH-responsive manners to the P3 micelles. Herein, the pH-responsibility of NCL-P3 micelles was measured by fluorescence spectroscopy with pyrene as the fluorescence probe, the I_{337}/I_{333} value of pyrene were plotted against the pH values to get the I_{337}/I_{333}-pH curve (Fig. S3†), with pH of 7.0–8.0, I_{337}/I_{333} of the pyrene-loaded NCL-P3 only slightly changed, indicating the NCL-P3 micelles are stable within this pH range. A drastic decreasing of I_{337}/I_{333} was observed when pH dropped from 7.0 to 5.6, suggesting the dissociation of NCL-P3 micelles, which due to the protonation-induced hydrophobicity–hydrophilicity conversion of PDPA. When pH value continuing dropped lower than 5.6, the I_{337}/I_{333} reached a platform, indicating the totally dissociation of NCL-P3 micelles. The pH-responsibility of NCL-P3 micelles also confirmed by DLS, as shown in Fig. 4, under neutral condition (pH 7.4), the average particle size of NCL-P3 micelles were about 50 nm, while under acidic condition (pH 5.0), the particle size drastically dropped to ~10 nm. The fluorescent and DLS assay results demonstrated the pH-responsive manners of NCL-P3.

By contrast, the pH-responsive properties of cystamine linker-containing SCL-P3 is different from that of NCL-P3 micelles. As the DLS curves shown in Fig. 5, the SCL-P3 micelles presented as small size nanoparticles (~56 nm) under pH 7.4, when pH dropped to 5.0, the particles size drastically increased to >200 nm along with broader size distribution, indicating the proton-induced swelling of SCL-P3 micelles. Notably, compare to the proton-induced dissociation of NCL-P3, the shell-crosslinked SCL-P3 micelles showed proton-induced swelling properties, implying that the cystamine crosslinking could effectively prevent complete dissociation of the micelles. To confirm the proton-induced swelling mechanism, ^{1}H NMR spectra of the SCL-P3 micelles (in D_2O) under pH = 5.0 and 7.4 were measured (Fig. 6), under neutral pH of 7.4,

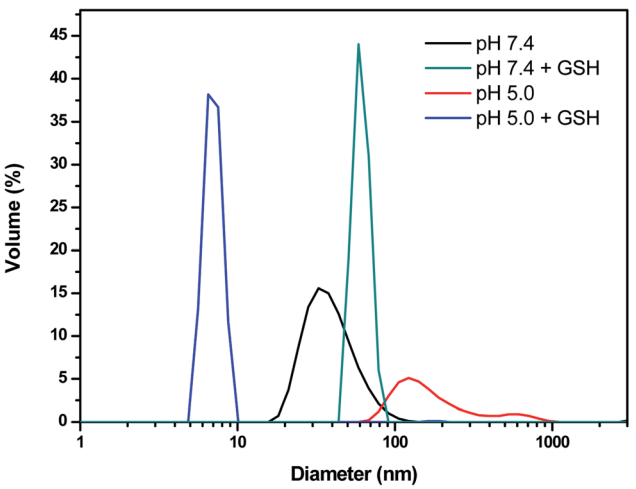

Fig. 5 Particle size and distribution of the SCL-P3 micelles in aqueous solution under different pH and bioreduction (GSH) environment. GSH concentration is 10 mM.

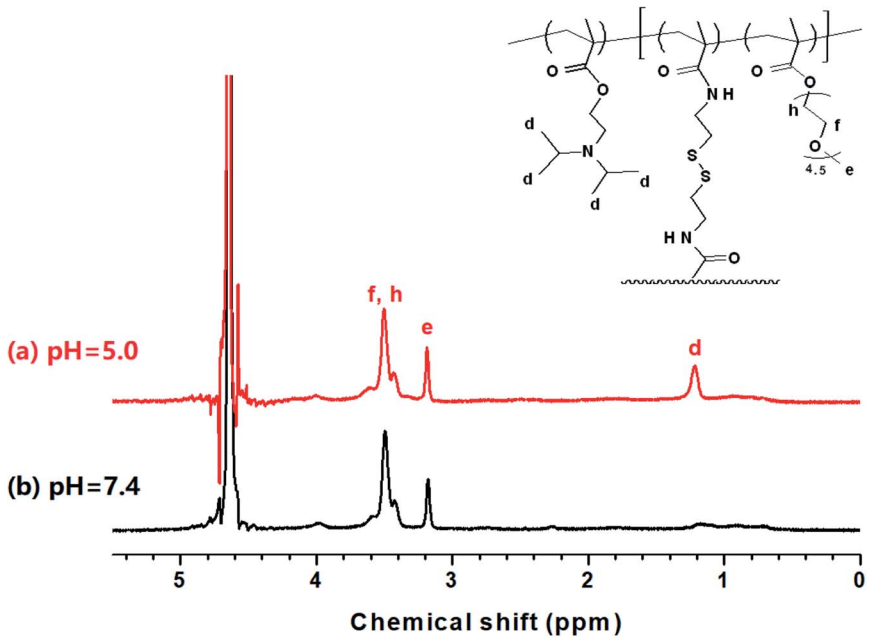

Fig. 6 ^{1}H NMR spectra of the SCL-P3 micelles under pH 5.0 (a) and pH 7.4 (b) in aqueous solution (D_2O).

almost no proton signals of isopropyl (iPr_2N) groups on PDPA could be clearly observed, which due to the imbedded PDPA hydrophobic core was totally shielded by hydrophilic P(NMS-*co*-OEG) "shell". When the solution pH dropped to 5.0, the isopropyl proton signals at 1.18–1.30 ppm in D_2O could be clearly observed, implying the protonation of PDPA caused the hydrophobicity–hydrophilicity conversion, thus increased the exposure of isopropyl groups on the outlayer of SCL-P3. Moreover, the protonation of SCL-P3 micelles under acidic conditions was also confirmed by zeta potential measurement (Fig. S4†).

We further examined the redox-responsibility of cystamine-containing SCL-P3 (Fig. 5), under the redox circumstances (10 mM GSH, pH 7.4), the particles sizes increased to ~85 nm with high PDI (~0.9), implying breakdown of disulfide cross-linkers caused the formation of loose-structured micelles. Notably, under co-existence of pH/redox-stimuli factors (pH 5.0 + 10 mM GSH), the SCL-P3 micelles almost completely dissociated into small fragments (~10 nm) with high PDI (~0.9), indicating that the SCL-P3 micelles possess remarkable pH/redox-dual responsive properties. The propose mechanisms were illustrated in Scheme 2.

3.5. The application of NCL-P3 and SCL-P3 micelles as smart nanomaterials for drug delivery

To evaluate the applicability of NCL-P3 and SCL-P3 as pH/redox dual-responsive "smart" nanomaterials in drug delivery application, camptothecin (CPT), an anti-tumor agent which interferes intracellular DNA replication/transcription by inhibiting the DNA topoisomerase,[38,39] was used as a model drug. Herein, we first prepared the CPT-loaded NCL-P3 micelles by self-assembly of P3 polymer with CPT (10% w/w), which was further crosslinked with cystamine (cystamine : NMS moiety, 1 : 2 molar ratio) to obtain the CPT-loaded SCL-P3 micelles.

The average particle size and distribution (PDI) of the micelles were measured by DLS analysis (Table 3 and Fig. S5†). The CPT-loaded NCL-P3 and SCL-P3 micelles both have small particle sizes (<100 nm) with low PDI (0.19–0.22). CPT-loaded SCL-P3 micelles showed a bit smaller particle size (68.7 nm) than that of CPT-loaded NCL-P3 (85.8 nm), indicating the cystamine crosslinking could condense the CPT-loaded micelles, which might be benefit for improving the micellar stability and enhancing the cellular uptake efficiency. Drug loading content (DLC) and drug loading efficiency (DLE) were determined by UV-vis spectrometer (Table 3) with CPT

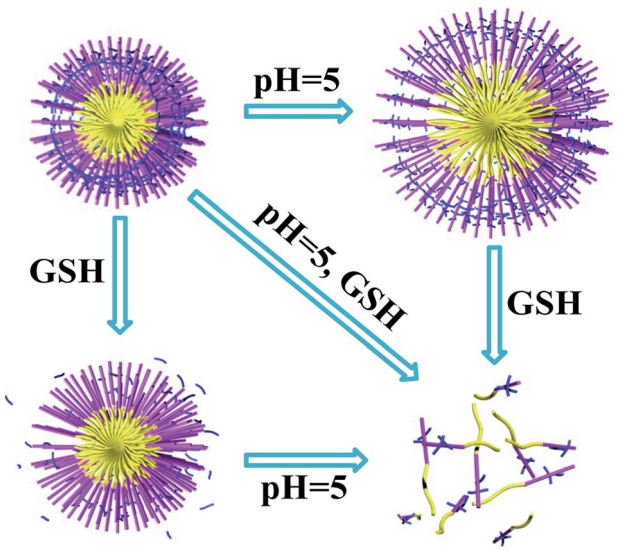

Scheme 2 The pH/redox-dual responsive properties of the SCL-P3 micelles (pH = 5, 10 mM GSH).

Table 3 Physico-chemical characteristics of the CPT-loaded NCL-P3 and SCL-P3 micelles

Sample	D_h[a] (nm)	PDI[a]	DLC[b] (wt%)	DLE[b] (wt%)
CPT-NCL-P3 micelles	85.8 ± 0.9	0.19 ± 0.05	1.4	15.2
CPT-SCL-P3 micelles	68.7 ± 0.6	0.22 ± 0.03	4.5	64.1

[a] Hydrodynamic diameters and particle size distribution of the CPT-loaded NCL-P3 and SCL-P3 micelles were determined by DLS using Zetasizer Nano-ZS (Malvern Instruments) at 25 °C in PBS buffer. [b] Drug loading content (DLC) and drug loading efficiency (DLE) were accordingly determined by UV-vis spectrometer.

calibration curves (Fig. S6†). The NCL micelles are not efficient nanocarriers for loading CPT due to the limited hydrophobicity of PDPA core and relatively "loose" micelle structure, the CPT loading capacity in the prepared NCL micelles is only 1.4% after dialysis. We anticipated that, cystamine cross-linking of the micelles could lead to the formation of condensed micelle payloads, and then improve the CPT-loading capacity, reduce the diffusion of CPT and increase the stability of the CPT-loaded micelles. Compare to the CPT-loading of NCL-P3 (DLC: 1.4%; DLE: 15.2%), SCL-P3 micelles (DLC: 4.5%; DLE 64.1%) showed remarkably enhanced CPT-loading capability. The results implied that *in situ* cystamine crosslinking of the CPT-loaded NCL-P3 micelles would greatly enhance the CPT-loading capability by providing a strengthened and stabilized "shell". Based on the CPT-loading results, the CPT-releasing properties of the CPT-loaded NCL-P3 and SCL-P3 micelles in PBS solution (pH = 7.4, 37 °C) were investigated by monitoring the fluorescence intensity of CPT, as shown in Fig. 7, the CPT-loaded NCL-P3 showed relative fast CPT release rate and higher accumulated CPT releasing amount of 61.3%, while CPT-loaded SCL-P3 showed slower CPT releasing and lower accumulated CPT releasing amount of 44.3%, indicating that the cystamine crosslinking could be used as a "valve" to control the CPT releasing and the kinetic stability of the micelles.

The *in vitro* pH/redox-triggered CPT release profiles of CPT-loaded SCL-P3 micelles were shown in Fig. 8. under the neutral condition (pH = 7.4, without GSH), CPT-loaded SCL-P3 micelles showed lower CPT release rates and lower accumulated release amount (44.3%) of CPT after 48 h incubation, when the pH rising to 5.0 (without GSH), faster CPT releasing and higher accumulated release amount of CPT at 54.6% (48 h) were observed. The pH-responsive CPT releasing could be attributed to the protonation-induced swelling and hydrophobicity–hydrophilicity conversion of CPT-loaded SCL-P3 micelles. Moreover, in the presence of redox agent (10 mM GSH, pH = 7.4), higher accumulated release amount (62.3%) of CPT was observed. The bioreduction-responsive effect is due to the GSH-cleavage of cystamine linkers in the micellar "shell". Notably, a synergistic CPT releasing effect were observed in the coexistence of pH/redox-stimuli factors (pH 5.0 + 10 mM GSH), which lead to the highest accumulated release amount (73.0%) of CPT. The pH-redox dual-responsive properties of CPT-loaded SCL-P3 micelles might be benefit for the intracellular lysosomal release of the loaded CPT within tumor cells.

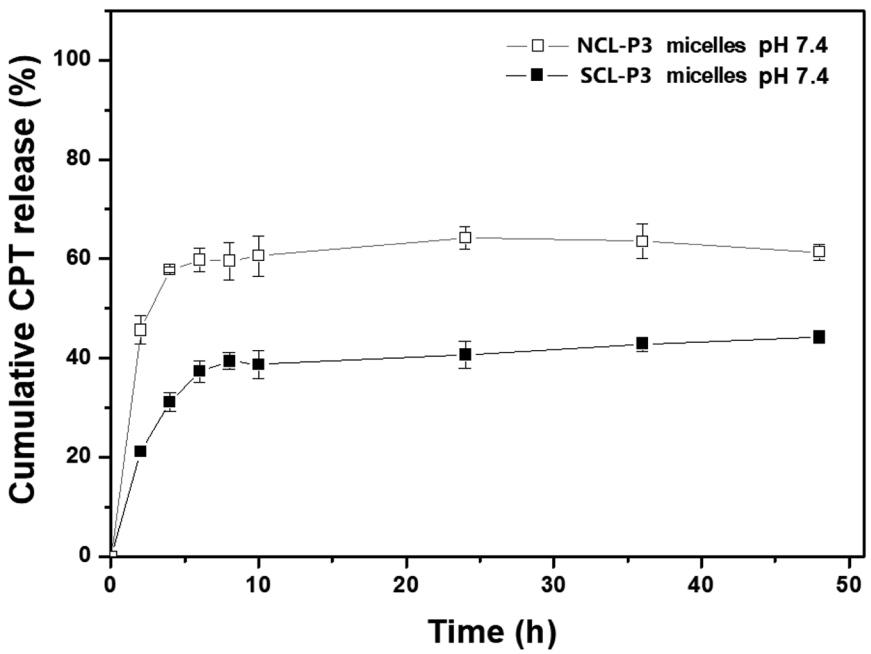

Fig. 7 CPT release under pH 7.4 in PBS solution for the CPT-loaded NCL-P3 and SCL-P3 micelles.

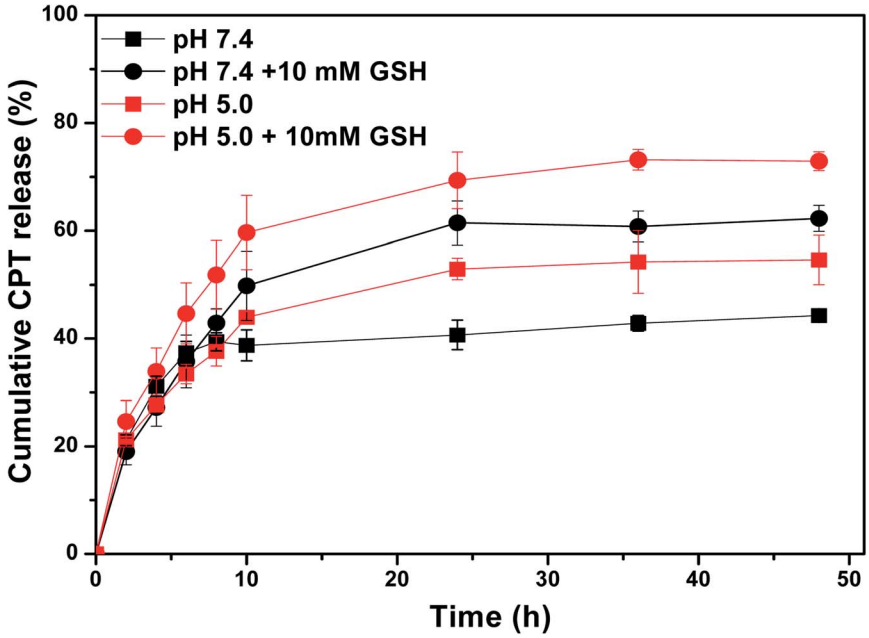

Fig. 8 CPT release profiles of the CPT-loaded SCL-P3 micelles under different pH/redox conditions (pH 5.0, pH 7.4, pH 5.0 + 10 mM GSH and pH 7.4 + 10 mM GSH).

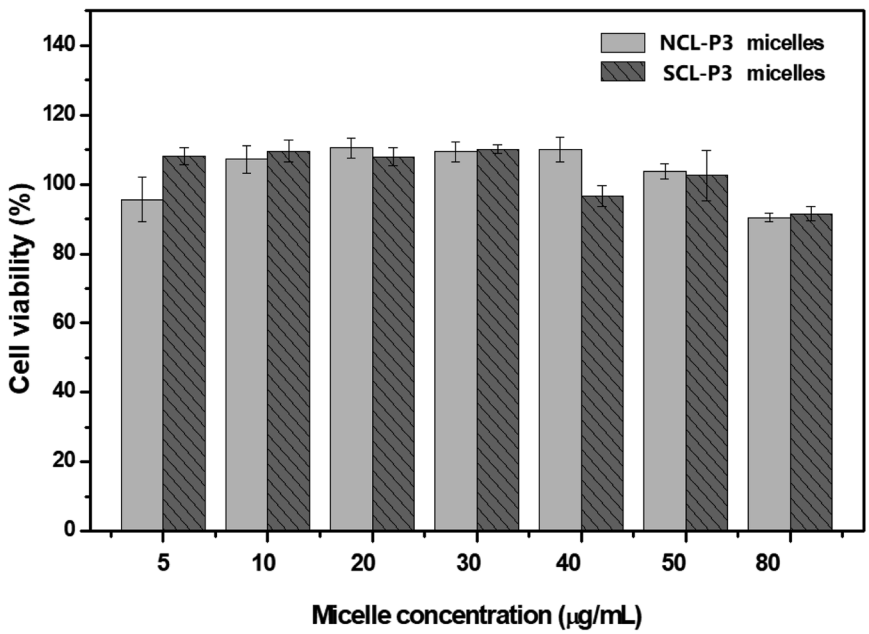

Fig. 9 Relative viability of H1299 cells under various dosages for the NCL-P3 and SCL-P3 micelles by MTT assay.

On the other hand, the biocompatibility of polymeric micelles is an important prerequisite for their application as safe drug delivery nanocarriers. Thus, the cytotoxicity of uncrosslinked NCL-P3 micelles and shell crosslinked SCL-P3 micelles on H1299 cells under various concentrations was further evaluated by MTT assay, and the results are shown in Fig. 9. It could be found that the relative H1299 cell viability were higher than 85.1% after treated with the NCL-P3 and SCL-P3 micelles at the concentration range of 5–80 μg mL^{-1}, indicating that the uncrosslinked and crosslinked micelles were low toxic and biocompatible carriers for drug delivery application.

4. Conclusion

In sum, we designed and prepared a series of well-defined amphiphilic PDPA-*b*-P(NMS-*co*-OEG) diblock terpolymers *via* RAFT polymerization strategy. They are able to self-assembled

into polymeric NCL nanomicelles, which could be *in situ* crosslinked with cystamine to prepare SCL micelles. Using P3 as an optimized polymer, SCL-P3 micelles were prepared, which demonstrated remarkable pH/redox dual responsive manners. The SCL-P3 micelles tend to swell at pH 5.0 and 10 mM GSH and almost totally dissociated under a combination of GSH/pH. For drug delivery application, CPT-loaded SCL-P3 micelles were prepared and showed much higher CPT-loading capability than the NCL-P3 counterparts. Notably, the SCL-P3 micelles showed good pH/redox-dual responsive CPT release properties. Moreover, the results elicited that, by properly introducing pH/redox-responsive building blocks into the polymer micelles, stabilized, controllable and synergistic pH/redox-dual responsive nanomaterials could be achieved and employed as "smart" nanocarriers towards drug delivery applications.

Conflicts of interest

There are no conflicts to declare.

Acknowledgements

The authors are indebted to the financial supports partially from the National Natural Science Foundation of China (21002116 and 21372251). Dr Ruilong Sheng appreciates ARDITI-Agência Regional para o Desenvolvimento da Investigação Tecnologia e Inovação, through the project M1420-01-0145-FEDER-000005-Centro de Química da Madeira-CQM$^+$ (Madeira 14-20), ARDITI-2017-ISG-003, FCT-Fundação para a Ciência e a Tecnologia (project PEst-OE/QUI/UI0674/2019, CQM, Portuguese Government funds), and project PROEQUI PRAM-Reforço do Investimento em Equipamentos e Infraestruturas Científicas na RAM (M1420-01-0145-FEDER-000008) for sponsorship. Dr Zhao Wang thanks the foundation support from Jinling Institute of Technology (Project No.: jit-b-201828).

References

1 E. R. Gillies and J. M. Fréchet, pH-responsive copolymer assemblies for controlled release of doxorubicin, *Bioconjugate Chem.*, 2005, **16**, 361–368.
2 R. Jain, S. M. Standley and J. M. Frechet, Synthesis and degradation of pH-sensitive linear poly(amidoamine)s, *Macromolecules*, 2007, **40**, 452–457.
3 E. M. Bachelder, T. T. Beaudette, K. E. Broaders, J. Dashe and J. M. Fréchet, Acetal-derivatized dextran: an acid-responsive biodegradable material for therapeutic applications, *J. Am. Chem. Soc.*, 2008, **130**, 10494–10495.
4 T. R. Daniels, T. Delgado, J. A. Rodriguez, G. Helguera and M. L. Penichet, The transferrin receptor part I: biology and targeting with cytotoxic antibodies for the treatment of cancer, *Clin. Immunol.*, 2006, **121**, 144–158.
5 J. KwonáOh, A dual location stimuli-responsive degradation strategy of block copolymer nanocarriers for accelerated release, *Chem. Commun.*, 2013, **49**, 7534–7536.
6 S.-M. Lee, R. W. Ahn, F. Chen, A. J. Fought, T. V. O'Halloran, V. L. Cryns and S. T. Nguyen, Biological evaluation of pH-responsive polymer-caged nanobins for breast cancer therapy, *ACS Nano*, 2010, **4**, 4971–4978.
7 J. You, G. Zhang and C. Li, Exceptionally high payload of doxorubicin in hollow gold nanospheres for near-infrared light-triggered drug release, *ACS Nano*, 2010, **4**, 1033–1041.
8 M. Talelli, C. J. Rijcken, T. Lammers, P. R. Seevinck, G. Storm, C. F. van Nostrum and W. E. Hennink, Superparamagnetic iron oxide nanoparticles encapsulated in biodegradable thermosensitive polymeric micelles: toward a targeted nanomedicine suitable for image-guided drug delivery, *Langmuir*, 2009, **25**, 2060–2067.
9 A. J. Harnoy, I. Rosenbaum, E. Tirosh, Y. Ebenstein, R. Shaharabani, R. Beck and R. J. Amir, Enzyme-Responsive Amphiphilic PEG-dendron Hybrids and their Assembly into Smart Micellar Nanocarriers, *J. Am. Chem. Soc.*, 2014, **136**, 7531–7534.
10 T.-H. Ku, M.-P. Chien, M. P. Thompson, R. S. Sinkovits, N. H. Olson, T. S. Baker and N. C. Gianneschi, Controlling and switching the morphology of micellar nanoparticles with enzymes, *J. Am. Chem. Soc.*, 2011, **133**, 8392–8395.
11 K. Engin, D. Leeper, J. Cater, A. Thistlethwaite, L. Tupchong and J. McFarlane, Extracellular pH distribution in human tumours, *Int. J. Hyperthermia*, 1995, **11**, 211–216.
12 Y. Bae, W.-D. Jang, N. Nishiyama, S. Fukushima and K. Kataoka, Multifunctional polymeric micelles with folate-mediated cancer cell targeting and pH-triggered drug releasing properties for active intracellular drug delivery, *Mol. BioSyst.*, 2005, **1**, 242–250.
13 Y. Bae, S. Fukushima, A. Harada and K. Kataoka, Design of environment-sensitive supramolecular assemblies for intracellular drug delivery: polymeric micelles that are responsive to intracellular pH change, *Angew. Chem., Int. Ed.*, 2003, **42**, 4640–4643.
14 Y. Du, W. Chen, M. Zheng, F. Meng and Z. Zhong, pH-sensitive degradable chimaeric polymersomes for the intracellular release of doxorubicin hydrochloride, *Biomaterials*, 2012, **33**, 7291–7299.
15 Y. Q. Yang, B. Zhao, Z. D. Li, W. J. Lin, C. Y. Zhang, X. D. Guo, J. F. Wang and L. J. Zhang, pH-sensitive micelles self-assembled from multi-arm star triblock co-polymers poly(ε-caprolactone)-b-poly (2-(diethylamino) ethyl methacrylate)-b-poly (poly(ethylene glycol) methyl ether methacrylate) for controlled anticancer drug delivery, *Acta Biomater.*, 2013, **9**, 7679–7690.
16 F. C. Giacomelli, P. Stepánek, C. Giacomelli, V. Schmidt, E. Jäger, A. Jäger and K. Ulbrich, pH-triggered block copolymer micelles based on a pH-responsive PDPA (poly [2-(diisopropylamino)ethyl methacrylate]) inner core and a PEO (poly(ethylene oxide)) outer shell as a potential tool for the cancer therapy, *Soft Matter*, 2011, **7**, 9316–9325.
17 K. Liang, G. K. Such, Z. Zhu, S. J. Dodds, A. P. Johnston, J. Cui, H. Ejima and F. Caruso, Engineering cellular degradation of multilayered capsules through controlled cross-linking, *ACS Nano*, 2012, **6**, 10186–10194.
18 H. Yu, Y. Zou, Y. Wang, X. Huang, G. Huang, B. D. Sumer, D. A. Boothman and J. Gao, Overcoming endosomal barrier by amphotericin B-loaded dual pH-responsive

PDMA-b-PDPA micelleplexes for siRNA delivery, *ACS Nano*, 2011, **5**, 9246–9255.

19 S. Li, W. Wu, K. M. Xiu, F. J. Xu, Z. M. Li and J. S. Li, Doxorubicin Loaded pH-Responsive Micelles Capable of Rapid Intracellular Drug Release for Potential Tumor Therapy, *J. Biomed. Nanotechnol.*, 2014, **10**, 1480–1489.

20 M. Licciardi, G. Giammona, J. Du, S. P. Armes, Y. Tang and A. L. Lewis, New folate-functionalized biocompatible block copolymer micelles as potential anti-cancer drug delivery systems, *Polymer*, 2006, **47**, 2946–2955.

21 H. Yu, Z. Xu, D. Wang, X. Chen, Z. Zhang, Q. Yin and Y. Li, Intracellular pH-activated PEG-b-PDPA wormlike micelles for hydrophobic drug delivery, *Polym. Chem.*, 2013, **4**, 5052–5055.

22 Y. H. Bae and H. Yin, Stability issues of polymeric micelles, *J. Controlled Release*, 2008, **131**, 2–4.

23 K. B. Thurmond, T. Kowalewski and K. L. Wooley, Water-soluble knedel-like structures: the preparation of shell-cross-linked small particles, *J. Am. Chem. Soc.*, 1996, **118**, 7239–7240.

24 K. B. Thurmond, T. Kowalewski and K. L. Wooley, Shell cross-linked knedels: a synthetic study of the factors affecting the dimensions and properties of amphiphilic core-shell nanospheres, *J. Am. Chem. Soc.*, 1997, **119**, 6656–6665.

25 Y. Cheng, C. He, C. Xiao, J. Ding, K. Ren, S. Yu, X. Zhuang and X. Chen, Reduction-responsive cross-linked micelles based on PEGylated polypeptides prepared via click chemistry, *Polym. Chem.*, 2013, **4**, 3851–3858.

26 J. Dai, S. Lin, D. Cheng, S. Zou and X. Shuai, Interlayer-Crosslinked Micelle with Partially Hydrated Core Showing Reduction and pH Dual Sensitivity for Pinpointed Intracellular Drug Release, *Angew. Chem., Int. Ed.*, 2011, **50**, 9404–9408.

27 A. H. Baugher, J. M. Goetz, L. M. McDowell, H. Huang, K. L. Wooley and J. Schaefer, Location of fluorotryptophan sequestered in an amphiphilic nanoparticle by rotational-echo double-resonance NMR, *Biophys. J.*, 1998, **75**, 2574–2576.

28 H.-M. Kao, A. D. Stefanescu, K. L. Wooley and J. Schaefer, Location of terminal groups of dendrimers in the solid state by rotational-echo double-resonance NMR, *Macromolecules*, 2000, **33**, 6214–6216.

29 H.-M. Kao, R. D. O'Connor, A. K. Mehta, H. Huang, B. Poliks, K. L. Wooley and J. Schaefer, Location of cholic acid sequestered by core–shell nanoparticles using REDOR NMR, *Macromolecules*, 2001, **34**, 544–546.

30 K. A. Davis and K. S. Anseth, Controlled release from crosslinked degradable networks, *Crit. Rev. Ther. Drug Carrier Syst.*, 2002, **19**, 385–423.

31 K. S. Murthy, Q. Ma, C. G. Clark Jr, E. E. Remsen and K. L. Wooley, Fundamental design aspects of amphiphilic shell-crosslinked nanoparticles for controlled release applications, *Chem. Commun.*, 2001, 773–774.

32 S. J. Lee, K. H. Min, H. J. Lee, A. N. Koo, H. P. Rim, B. J. Jeon, S. Y. Jeong, J. S. Heo and S. C. Lee, Ketal cross-linked poly(ethylene glycol)-poly(amino acid)s copolymer micelles for efficient intracellular delivery of doxorubicin, *Biomacromolecules*, 2011, **12**, 1224–1233.

33 Y. Li, B. S. Lokitz, S. P. Armes and C. L. McCormick, Synthesis of reversible shell cross-linked micelles for controlled release of bioactive agents, *Macromolecules*, 2006, **39**, 2726–2728.

34 X. Hu, H. Li, S. Luo, T. Liu, Y. Jiang and S. Liu, Thiol and pH dual-responsive dynamic covalent shell cross-linked micelles for triggered release of chemotherapeutic drugs, *Polym. Chem.*, 2013, **4**, 695–706.

35 X. Hu, J. Tian, T. Liu, G. Zhang and S. Liu, Photo-triggered release of caged camptothecin prodrugs from dually responsive shell cross-linked micelles, *Macromolecules*, 2013, **46**, 6243–6256.

36 S. Zhai, X. Hu, Y. Hu, B. Wu and D. Xing, Visible light-induced crosslinking and physiological stabilization of diselenide-rich nanoparticles for redox-responsive drug release and combination chemotherapy, *Biomaterials*, 2017, **121**, 41–54.

37 Y. Pan, H. Bao, N. G. Sahoo, T. Wu and L. Li, Water-Soluble Poly(*N*-isopropylacrylamide)–Graphene Sheets Synthesized *via* Click Chemistry for Drug Delivery, *Adv. Funct. Mater.*, 2011, **21**, 2754–2763.

38 X. Li, X. Kong, J. Zhang, Y. Wang, Y. Wang, S. Shi, G. Guo, F. Luo, X. Zhao and Y. Wei, A novel composite hydrogel based on chitosan and inorganic phosphate for local drug delivery of camptothecin nanocolloids, *J. Pharm. Sci.*, 2011, **100**, 232–241.

39 D.-L. Tang, F. Song, C. Chen, X.-L. Wang and Y.-Z. Wang, A pH-responsive chitosan-b-poly(p-dioxanone) nanocarrier: formation and efficient antitumor drug delivery, *Nanotechnology*, 2013, **24**, 145101.